Kaplan–Meier method [27]. Univariate survival analysis was performed using the log-rank test and multivariate survival analysis was performed using Cox proportional hazard regression [28]. Independent prognostic factors were evaluated using the Cox's proportional hazards regression model. A p-value difference of <0.01 were considered to be significant. Statistical analyses were performed using Dr. SPSS II (version 11.01) (IBM, Armonk, NY, USA).

3 Results

3.1 Depletion of NPM inhibited proliferation of Ewing's sarcoma cells

There is controversy regarding the effects of NPM on cells; it promotes oncogenesis, and in contrast suppresses tumor progression, depending on conditions [29]. Therefore, we first investigated the functional significance of NPM expression in Ewing's sarcoma. Compared with the control, stable transfection with NPM-specific shRNA successfully reduced the levels of expression of NPM mRNA and protein in three Ewing's sarcoma cell lines (Fig. 1A and B, respectively). Further, proliferation of three Ewing's sarcoma cell lines was significantly reduced (Fig. 1C), while tumor cell invasiveness was not affected (Supporting Information Fig. 1). Because NPM promoted the invasiveness of colorectal cancer cells [30], the influence of NPM on invasion may depend on cell type. Reduced cell proliferation was associated with the down-regulation of the levels of cyclin D1 (Fig. 1D), suggesting that the cell cycle was negatively regulated by the depletion of NPM. These observations are consistent with those reported by others [31]. The association of NPM with poor prognosis of patients with Ewing's sarcoma may stem from the ability of NPM to stimulate cell proliferation.

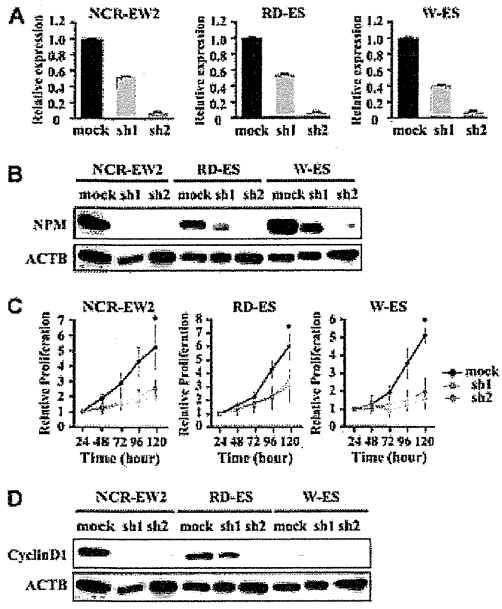

Figure 1. Suppression of the expression of NPM inhibited proliferation of Ewing's sarcoma cells. The Ewing sarcoma cell lines, NCR-EW2 [21], RD-ES, and W-ES [22], were transfected with NPM shRNAs or a negative control. (A) RT-PCR analysis shows the decrease of *NPM1* mRNA expression by two different shRNAs. (B) Western blots show the decrease of NPM expression induced by NPM shRNAs. (C) The number of cells in a defined area was counted at 24, 48, 72, 96, and 120 h after seeding. The examination was repeated three times, and mean and standard deviation (error bars) were calculated. (*: Student t test between transfected shRNA-NPM vs. mock, p <0.01). (D) Expression of Cyclin D1 in NPM-suppressed and control cells.

3.2 Identification of 106 NPM complex proteins using interactome analysis

The workflow of the FLAG-tag-based protein complex purification is illustrated in Fig. 2A. Three Ewing's sarcoma cell lines were stably transfected with the FLAG-tagged NPM expression vector, and cellular proteins that were involved in the NPM complex were isolated using the FLAG-tag specific antibody conjugated to agarose beads. The immunoprecipitated proteins were separated according to their molecular weights by SDS-PAGE, cut into 24 gels, and recovered as peptides by in-gel digestion by trypsin. The advantages of fractionating proteins prior to MS were established [32–37]. Figure 2B demonstrates the appearance of SDS-PAGE gels including separated protein complexes; nonspecifically recovered proteins were observed in the control samples. By subtracting identified proteins between FLAG-tagged NPM-transfected cells and controls, the nonspecifically recovered proteins were excluded from further analysis. Consequently, 106 proteins were identified in Ewing's sarcoma cell lines (Fig. 2C and Supporting Information Table 1), 36 proteins were identified in three cell lines, 23 proteins in two (Table 1), and 47 proteins in one of the three (Supporting Information Table 3). Mass spectrometric data supporting the identification of proteins is provided in Supporting Information Table 2. The associations of the identified proteins with NPM were confirmed by immunoprecipitation-Western blotting for NUCL (Supporting Information Fig. 2). 2D-Western blotting suggested that the post-translational modification of each of these three Ewing's sarcoma cell lines was different (Supporting Information Fig. 3), suggesting unique interactions of the proteins in each cell line. The associations of 57 proteins with NPM are known and 49 proteins were newly identified as NPM-binding proteins in this study (Table 1, Supporting Information Table 3). The functional classifications of the 106 proteins are illustrated in Fig. 2D and summarized in Supporting Information Table 4. These proteins are involved in ribosome biogenesis, regulation of transcription or translation, protein folding, nucleosome assembly, mRNA/tRNA processing or splicing, cell cycle regulation, angiogenesis, cell adhesion, and protein kinase cascades. These findings suggest that multifunctional roles of NPM may

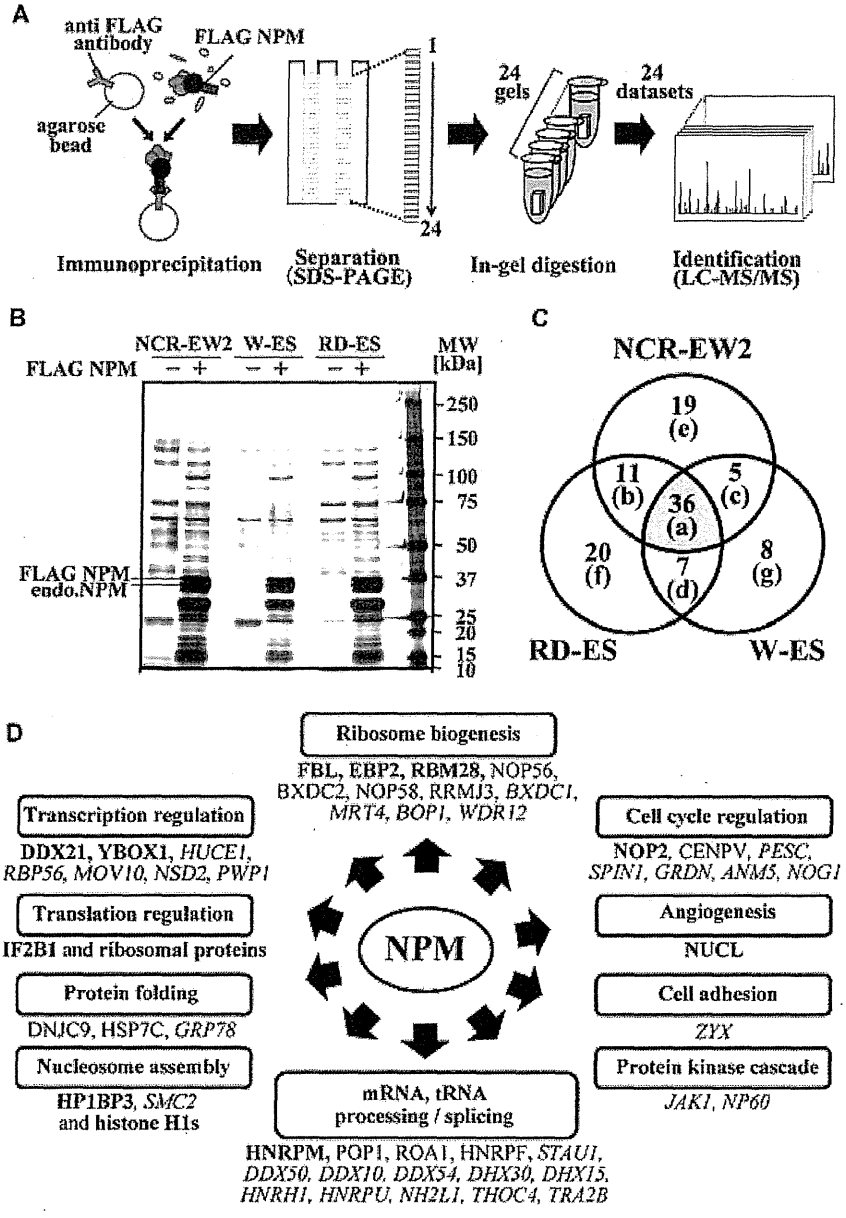

Figure 2. Identification of NPM-binding proteins. (A) Experimental workflow for the identification of the proteins in the NPM complex. (B) Overview of the precipitated proteins. (C) Venn diagrams of a number of NPM-binding proteins identified in Ewing's sarcoma cell lines. One hundred six proteins were identified. The letter in brackets corresponds to the category indicated in Supporting Information Table 5 in which the proteins are listed with their accession number and name. (D) Functional classification of the proteins in the NPM protein complex. Bold text indicates the proteins identified in all three cell lines. Plain and italic text indicates the proteins identified in 2 and 1 cell line, respectively. The data to support these classifications are shown in Supporting Information Table 4.

stem from its interactions with other proteins with various properties.

3.3 Proteins associated with malignancies

We found that the expression levels of 12 of the 106 proteins are known to correlate with poor prognosis of patients with malignancies (Fig. 3, Supporting Information Table 5). The functional properties of these 12 proteins may contribute to malignant potential of tumor cells. Further, NPM promotes cell proliferation and may also contribute to the malignant properties of Ewing's sarcoma cells by interacting with these proteins.

3.4 Meta-analysis confirmed the prognostic value of proteins in the NPM protein complex

To explore the clinical utility of the proteins, the survival of 32 patients with Ewing's sarcoma was assessed using meta-analysis. Among the 106 proteins, the mRNA expression levels of 103 genes in these patients were obtained from a transcriptome study (GSE17674) [38]. The clinical and pathological data for the 32 patients and the mRNA expression data of the 103 genes are summarized in Supporting Information Tables 6 and 7, respectively. We selected genes whose AUC values were greater than 0.6 between the patient groups who had different survival periods. According to the

Table 1. NPM binding proteins identified in more than two Ewing's sarcoma cell lines

Related major pathways/ processes[a]	Protein name[b]	Gene name[b]	Description	Reported[c]	Cell line[d]			AUC[e]	*p*-value[f]		Fluctuation[g]
					NCR-EW2	RD-ES	W-ES		OS	DFS	
Ribosome biogenesis	FBRL	FBL	rRNA 2~-O-methyl-transferase fibrillarin	+	•	•	•	0.521	0.7908	0.2483	Negative
	EBP2	EBNA1BP2	Probable rRNA-processing protein EBP2		•	•	•	0.596	0.0513	0.0739	Positive
	RBM28	RBM28	RNA-binding protein 28		•	•	•	0.548	0.0288	0.0222	Positive
	NOP56	NOP56	Nucleolar protein 56	+	•	•		**0.771**	**0.0004**	**0.0031**	Positive
	BXDC2	BXDC2	Brix domain-containing protein 2		•		•	**0.633**	**0.0041**	0.0378	Positive
	NOP58	NOP58	Nucleolar protein 58		•		•	0.575	0.0437	0.0454	Positive
	RRMJ3	FTSJ3	Putative rRNA methyltransferase 3			•	•	**0.692**	0.0596	**0.0095**	Negative
Cell cycle regulation	NOP2	NOP2	Putative ribosomal RNA methyltransferase NOP2	+	•	•	•	**0.635**	0.0213	**0.0068**	Positive
	CENPV	CENPV	Centromere protein V		•	•		**0.633**	**0.0024**	0.1461	Positive
mRNA, tRNA processing / splicing	HNRPM	HNRNPM	Heterogeneous nuclear ribonucleoprotein M	+	•	•	•	0.521	0.2119	0.9769	Negative
	POP1	POP1	Ribonucleases P/MRP protein subunit POP1		•	•		0.575	0.7066	0.9691	Positive
	ROA1	HNRNPA1	Heterogeneous nuclear ribonucleoprotein A1	+	•	•		**0.604**	0.0912	0.1091	Negative
	HNRPF	HNRNPF	Heterogeneous nuclear ribonucleoprotein F		•	•		**0.617**	0.6659	0.1843	Negative
Protein folding	DNJC9	DNAJC9	DnaJ homolog subfamily C member 9		•	•		**0.658**	**0.0083**	0.0105	Negative
	HSP7C	HSPA8	Heat shock cognate 71 kDa protein			•	•	0.579	0.3731	0.2924	Negative
Nucleosome assembly	HP1B3	HP1BP3	Heterochromatin protein 1-binding protein 3		•	•	•	0.500	0.0460	0.1186	Positive
Transcription regulation	DDX21	DDX21	Nucleolar RNA helicase 2	+	•	•	•	**0.606**	0.2448	0.0353	Negative
	YBOX1	YBX1	Nuclease-sensitive element-binding protein 1	+	•	•	•	0.562	0.0388	0.3756	Positive
Angiogenesis	NUCL	NCL	Nucleolin	+	•	•	•	0.525	0.1848	0.7400	Positive
Translation regulation	IF2B1	IGF2BP1	Insulin-like growth factor 2 mRNA-binding protein 1		•	•		0.512	0.5504	0.2329	Positive
Ribosomal protein	RL13	RPL13	60S ribosomal protein L13	+	•	•	•	0.571	0.3179	0.2864	Negative
	RL13A	RPL13A	60S ribosomal protein L13a	+	•	•	•	**0.713**	0.3353	0.1110	Negative
	RL14	RPL14	60S ribosomal protein L14	+	•	•	•	0.537	0.2275	0.2684	Negative
	RL15	RPL15	60S ribosomal protein L15	+	•	•	•	**0.617**	0.3885	0.1675	Negative
	RL17	RPL17	60S ribosomal protein L17	+	•	•	•	0.596	0.2014	0.1454	Negative
	RL18	RPL18	60S ribosomal protein L18	+	•	•	•	**0.621**	0.6542	0.3756	Negative
	RL23A	RPL23A	60S ribosomal protein L23a	+	•	•	•	0.529	0.1838	0.0311	Negative
	RL27	RPL27	60S ribosomal protein L27	+	•	•	•	0.529	0.9184	0.0351	Positive
	RL3	RPL3	60S ribosomal protein L3	+	•	•	•	**0.713**	**0.0071**	**0.0016**	Negative
	RL30	RPL30	60S ribosomal protein L30	+	•	•	•	0.575	0.7869	0.4534	Negative
	RL32	RPL32	60S ribosomal protein L32	+	•	•	•	**0.625**	0.4302	0.3905	Negative
	RL4	RPL4	60S ribosomal protein L4	+	•	•	•	**0.704**	0.0850	0.0435	Negative
	RL6	RPL6	60S ribosomal protein L6	+	•	•	•	0.508	0.9079	0.2077	Positive
	RL7	RPL7	60S ribosomal protein L7	+	•	•	•	0.512	0.9790	0.7287	Positive
	RL7A	RPL7A	60S ribosomal protein L7a	+	•	•	•	**0.633**	0.0702	0.0082	Negative
	RL8	RPL8	60S ribosomal protein L8	+	•	•	•	0.525	0.7646	0.5000	Negative
	RLA0	RPLP0	60S acidic ribosomal protein P0	+	•	•	•	0.529	0.8234	0.6549	Negative
	RS13	RPS13	40S ribosomal protein S13	+	•	•	•	0.554	0.4203	0.1501	Negative

Continued

Table 1. *Continued*

Related major pathways/ processes[a]	Protein name[b]	Gene name[b]	Description	Reported[c]	Cell line[d]			AUC[e]	*p*-value[f]		Fluctuation[g]
					NCR-EW2	RD-ES	W-ES		OS	DFS	
	RS2	RPS2	40S ribosomal protein S2	+	•	•	•	0.554	0.9857	0.6958	Negative
	RS3A	RPS3A	40S ribosomal protein S3a	+	•	•	•	0.571	0.4237	0.1160	Negative
	RS6	RPS6	40S ribosomal protein S6	+	•	•	•	**0.617**	0.8714	0.4255	Negative
	RS8	RPS8	40S ribosomal protein S8	+	•	•	•	**0.617**	0.2232	0.0351	Negative
	RS9	RPS9	40S ribosomal protein S9	+	•	•	•	**0.604**	0.0876	0.0107	Negative
	RL1D1	RSL1D1	Ribosomal L1 domain-containing protein 1	+	•	•	•	0.500	0.4778	0.0500	Negative
	RL10A	RPL10A	60S ribosomal protein L10a	+	•	•	•	**0.646**	0.0460	**0.0009**	Negative
	RL21	RPL21	60S ribosomal protein L21	+	•	•		0.575	0.5540	0.3440	Negative
	RL31	RPL31	60S ribosomal protein L31	+	•	•		**0.733**	0.0957	**0.0057**	Negative
	RL34	RPL34	60S ribosomal protein L34	+	•	•		0.588	0.9630	0.7753	Negative
	RS14	RPS14	40S ribosomal protein S14	+	•	•		**0.633**	0.0307	0.0156	Negative
	RL12	RPL12	60S ribosomal protein L12	+	•		•	**0.713**	0.0459	0.0133	Negative
	RL18A	RPL18A	60S ribosomal protein L18a	+		•	•	0.604	0.6769	0.1172	Negative
	RL19	RPL19	60S ribosomal protein L19	+		•	•	0.567	0.3717	0.0904	Negative
	RL24	RPL24	60S ribosomal protein L24	+		•	•	0.567	0.4815	0.1058	Negative
	RLA2	RPLP2	60S acidic ribosomal protein P2	+		•	•	0.567	0.0507	0.0828	Positive
Histone	H10	H1F0	Histone H1.0	+	•	•	•	0.562	0.1008	0.1172	Negative
	H1X	H1FX	Histone H1x	+	•	•	•	0.567	0.1350	0.3832	Positive
	H14	HIST1H1E	Histone H1.4	+	•		•	**0.708**	**4E-03**	**0.0095**	Positive
	H13	HIST1H1D	Histone H1.3	+	•		•	0.575	0.1896	0.5762	Positive
	H15	HIST1H1B	Histone H1.5	+		•	•	0.592	0.3153	0.4694	Positive

a) The data supportive to classification are demonstrated in Supplementary Table 4.
b) Protein and gene names were derived from Swiss-Prot and NCBI nonredundant databases.
c) + indicates protein which was previous reported as NPM binding protein.
d) • indicates the cell line in which per NPM binding protein was identified.
e) AUC value was determined comparing patients with ≥3 years OS and < 3 years OS with R (version 2.6.0) and Epi package. Bold numbers indicate significant values (AUC > 0.6).
f) Bold numbers indicate significant values ($p < 0.01$).
g) Positive: expression was positively correlated with poor prognosis, negative: expression was negatively correlated with poor prognosis.

best cutoff value, we examined the survival curves and evaluated the significances using a log rank test. We found that six genes with elevated levels of expression (AUC >0.6) associated significantly (log rank test, p <0.01) with shorter OS and DFS. These included NOP56 (*NOP56*), RL3 (*RPL3*), H14 (*HIST1H1E*), CG050 (*C7orf50*), STAU1 (*SAU1*),and DDX50 (*DDX50*). Among them, *NOP56*, *RPL3*, and *HIST1H1E* were present in the NPM protein complex in three cell lines. The correlation of survival with the expression of these three genes is demonstrated in Fig. 4. Multivariate analysis demonstrated that they were independent prognostic factors in terms of OS, DFS, or both (Supporting Information Table 8). The survival curves and the results of multivariate analyses for *C7orf50*, *STAU1*, and *DDX50* are shown in Supporting Information Figure 4 and Supporting Information Table 8, respectively. Functional roles of these six genes in the response to treatments, cancer progression, and stress response are known (Supporting Information Table 9); while, their functional significances and clinical values were nor examined in Ewing's sarcoma.

4 Discussion

Studying the properties of candidate biomarkers may reveal new insights into tumor cell biology. First, because the correlations between biomarkers and disease phenotypes are statistically evaluated by analysis of clinical materials, we believe that it is reasonable to conclude a functional role of novel biomarkers. Second, we may be able to identify novel biomarker candidates from proteins that structurally and functionally interact with the existing biomarkers. As proteins may generally function with the other proteins through interactions, the biomarker-interacting proteins may also have clinical values. Based on these two hypotheses, we conducted an interactomic study for candidate biomarker proteins that directly and indirectly bind to NPM in Ewing's sarcoma cell lines.

We employed size fractionation before MS analysis. Prefractionation by SDS-PAGE has great advantages for observing greater numbers of protein compared to other separation techniques and is widely used to characterize protein

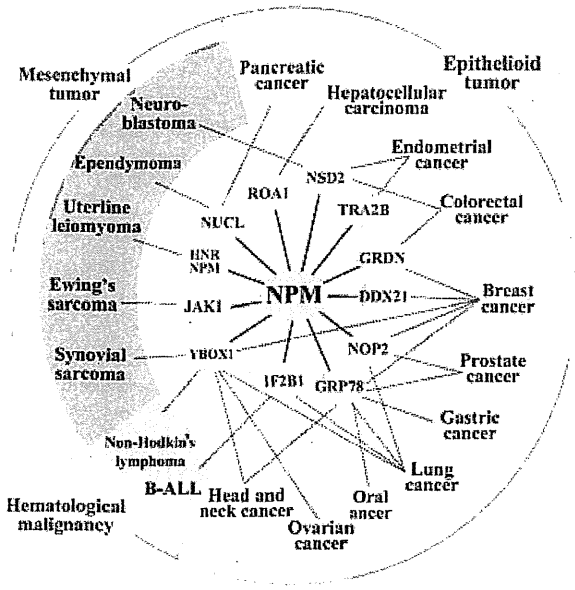

Figure 3. Prognostic bio-marker candidate NPM-binding proteins. The 14 NPM-binding proteins are known as prognostic biomarkers for various cancers. The reference data are summarized in Supporting Information Table 5. B-ALL: B-cell acute lymphoblastic leukemia.

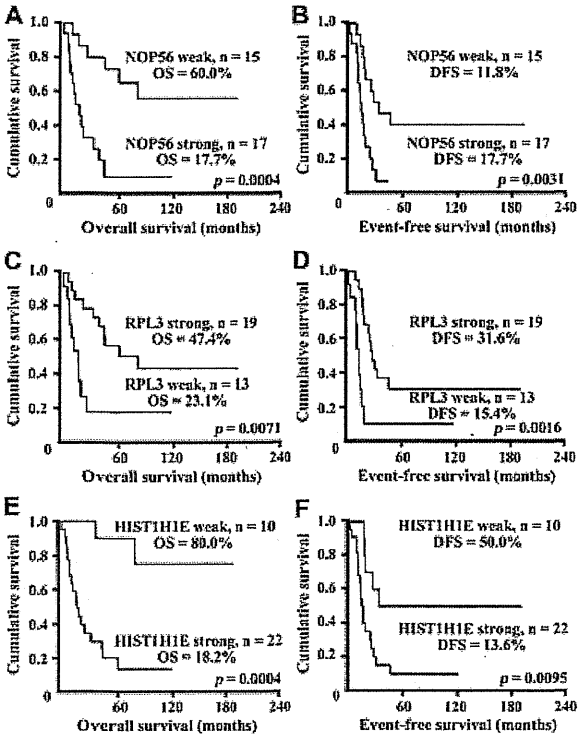

Figure 4. Relationship between the survival of Ewing's sarcoma patients and NPM-binding proteins identified in Ewing's sarcoma cell lines. Kaplan-Meier survival curves. Patients with high expression of *NOP56* (A, B), *RPL3* (C, D), and *HIST1H1E* (E, F) had significantly shorter OS and DFS (log rank *p*-value <0.01).

complexes in interactomic studies [33–37]. Gel-based size fractionation for the identification of proteins is superior to separation by liquid chromatography [32]. Jafari et al. compared gel-based protein separation techniques, including SDS-PAGE, IEF-IPG, and 2D-PAGE, for their ability to serve as fractionation techniques for MS analysis of a complex protein sample [39]. They reported that SDS-PAGE yielded the highest number of identifiable proteins.

By fractionating the co-immunoprecipitated proteins using SDS-PAGE before MS, we identified 106 proteins associated with NPM. Among them, 36, 23, and 47 were present in three, two, or one Ewing's sarcoma cell lines, respectively. The differential distribution of NPM complex proteins may reflect the posttranslational modification patterns of NPM, which differ among these three cell lines (Supporting Information Figure 2). Functional significances of posttranslational modifications of NPM may be approached by investigating the differential components of NPM protein complex in these cells.

Of the 106 proteins identified here, 12 are known as prognostic biomarkers for various malignancies (Fig. 3). Among the other 94 proteins, meta-analysis revealed that the mRNA expression levels of six proteins statistically correlated with prognosis. NOP56 (*NOP56*) and H14 (*HIST1H1E*) positively correlated with a shorter survival. In contrast, RL3 (*RPL3*) positively correlated with a favorable prognosis. These results are consistent with previous studies (Supporting Information Table 9). Our present results suggest that NPM might promote the functions of oncoproteins and repress the activities of tumor suppressors. Indeed, previous reports demonstrated that NPM is a coactivator of the oncoprotein NF-kB [40], and in contrast, it suppresses the functions of tumor suppressor ARF [41]. These observations may suggest that we may be able to discover novel biomarker candidates both for a favorable and poor prognosis using an interactomic approach.

There are limitations in the present interactome approach. First, it cannot distinguish between direct and indirect interacting partners of NPM. The identified proteins may contain both direct and indirect interacting proteins, and it is worth to distinguish them when considering the functional significances. Second, we used qualitative data to identify the proteins in the NPM protein complexes; the proteins detected specifically in the FLAG-tagged NPM transfected cells were selected for the further analysis. For the further investigation, it is worth considering the quantitative differences of identified proteins expressed in the three FLAG-tagged NPM transfected cells. The SILAC-based quantitative interactome analysis is a candidate approach for further studies [42]. Third, the identified proteins in this study included those with various cellular localizations [5]. NPM was observed in multiple cellular locations in Ewing's sarcoma cells, and it is worth investigating the location specific interactions for further understanding of NPM functions. Fourth, the expression level of mRNA does not always show concordance with that of protein, and it is a protein that functions and regulates phenotypes of cancer cells. Therefore, the correlations between gene expression and clinical information, that obtained by

meta-analysis, should be confirmed at the protein level, so that we can have mechanistic backgrounds of the observed correlation.

In conclusion, to examine the molecular functions underlying the association between NPM expression and poor prognosis of patients with Ewing's sarcoma, we employed an interactomic approach. The proteins in the NPM protein complex may function coordinately and contribute to the malignant behavior of Ewing's sarcoma cells. It is worth considering the general utility of the interactome approach in conjunction with meta-analysis for the discovery of biomarkers.

This work was supported by the National Cancer Center Research and Development Fund (23-A-10).

The authors have declared no conflict of interest.

5 References

[1] Epstein, R. J., *Eur. J. Cancer* 2009, *45*, 1111–1116.

[2] Kondo, T., Hirohashi, S., *Methods Mol. Biol.* 2009, *577*, 135–154.

[3] Cotterill, S. J., Ahrens, S., Paulussen, M., Jurgens, H. F., Voûte, P. A., Gadner, H., Craft, A. W., *J. Clin. Oncol.* 2000, *18*, 3108–3114.

[4] Kolb, E. A., Kushner, B. H., Gorlick, R., Laverdiere, C., Healey, J. H., LaQuaglia, M. P., Huvos, A. G., Qin, J., Vu, H. T., Wexler, L., Wolden, S., Meyers, P. A., *J. Clin. Oncol.* 2003, *21*, 3423–3430.

[5] Kikuta, K., Tochigi, N., Shimoda, T., Yabe, H., Morioka, H., Toyama, Y., Hosono, A., Beppu, Y., Kawai, A., Hirohashi, S., Kondo, T., *Clin. Cancer Res.* 2009, *15*, 2885–2894.

[6] Colombo, E., Alcalay, M., Pelicci, P. G., *Oncogene* 2011, *30*, 2595–2609.

[7] Morris, S. W., Kirstein, M. N., Valentine, M. B., Dittmer, K. G., Shapiro, D. N., Saltman, D. L., Look, A. T., *Science* 1994, *263*, 1281–1284.

[8] Falini, B., Mecucci, C., Tiacci, E., Alcalay, M., Rosati, R., Pasqualucci, L., La, Starza, R., Diverio, D., Colombo, E., Santucci, A., Bigerna, B., Pacini, R., Pucciarini, A., Liso, A., Vignetti, M., Fazi, P., Meani, N., Pettirossi, V., Saglio, G., Mandelli, F., Lo-Coco, F., Pelicci, P. G., Martelli, M. F., GIMEMA Acute Leukemia Working Party, *N. Engl. J. Med* 2005, *352*, 254–266.

[9] Subong, E. N., Shue, M. J., Epstein, J. I., Briggman, J. V., Chan, P. K., Partin, A. W., *Prostate* 1999, *39*, 298–304.

[10] Tanaka, M., Sasaki, H., Kino, I., Sugimura, T., Terada, M., *Cancer Res.* 1992, *52*, 3372–3377.

[11] Nozawa, Y., Van Belzen, N., Van der Made, A. C., Dinjens, W. N., Bosman, F. T., *J. Pathol.* 1996, *178*, 48–52.

[12] Zhang, Y., *Cell Cycle* 2004, *3*, 259–262.

[13] Tsui, K. H., Cheng, A. J., Chang, P. L., Pan, T. L., Yung, B. Y., *Urology* 2004, *64*, 839–844.

[14] Vidal, M., Cusick, M. E., Barabasi, A. L., *Cell* 2011, *144*, 986–998.

[15] Sun, J., Zhao, Z., *BMC Genomics* 2010, *11*(Suppl 3), S5.

[16] Lindstrom, M. S., *Biochem. Res. Int.* 2011, *2011*, 195–209.

[17] Llanos, S., Clark, P. A., Rowe, J., Peters, G., *Nat. Cell Biol.* 2001, *3*, 445–452.

[18] Colombo, E., Marine, J. C., Danovi, D., Falini, B., Pelicci, P. G., *Nat. Cell Biol.* 2002, *4*, 529–533.

[19] Li, Z., Boone, D., Hann, S. R., *Proc. Natl. Acad. Sci. USA* 2008, *105*, 18794–18799.

[20] Bertwistle, D., Sugimoto, M., Sherr, C. J., *Mol. Cell. Biol.* 2004, *24*, 985–996.

[21] Hara, S., Ishii, E., Tanaka, S., Yokoyama, J., Katsumata, K., Fujimoto, J., Hata, J., *Br. J. Cancer* 1989, *60*, 875–879.

[22] Fujii, Y., Nakagawa, Y., Hongo, T., Igarashi, Y., Aito, Y., Maeda, M., *Hum. Cell* 1989, *2*, 190–191.

[23] Kitamura, T., Koshino, Y., Shibata, F., Oki, T., Nakajima, H., Nosaka, T., Kumagai, H., *Exp. Hematol.* 2003, *31*, 1007–1014.

[24] Kondo, T., Hirohashi, S., *Nat. Protocols* 2007, *1*, 2940–2956.

[25] Creelman, C. D., Donaldson, W., *J. Exp. Psychol.* 1968, *77*, 514–516.

[26] Puri, A., Gulia, A., Jambhekar, N. A., Laskar, S., *J. Surg. Oncol.* 2012, *106*, 417–422.

[27] Kaplan, E., Meier, P., *J. Am. Stat. Assoc.* 1958, *53*, 457–481.

[28] Cox, D., *J. R. Stat. Soc.* 1972, *34*, 187–220.

[29] Di Fiore, P. P., *J. Cell Biol.* 2008, *182*, 7–9.

[30] Liu, Y., Zhang, F., Zhang, X. F., Qi, L. S., Yang, L., Guo, H., Zhang, N., *J. Biomed. Sci.* 2012, *19*, 53.

[31] Xiao, J., Zhang, Z., Chen, G. G., Zhang, M., Ding, Y., Fu, J., Li, M., Yun, J. P., *Cell Cycle* 2009, *8*, 889–895.

[32] Pernemalm, M., Orre, L. M., Lengqvist, J., Wikstrom, P., et al., *J. Proteome Res.* 2008, *7*, 2712–2722.

[33] Fang, X., Yoon, J. G., Li, L., Tsai, Y. S., Zheng, S., Hood, L., Goodlett, D. R., Foltz, G., Lin, B., *Proteomics* 2011, *11*, 921–934.

[34] Cottingham, K., *J. Proteome Res.* 2010, *9*, 1636.

[35] Fang, Y., Robinson, D. P., Foster, L. J., *J. Proteome Res.* 2010, *9*, 1902–1912.

[36] Piersma, S. R., Fiedler, U., Span, S., Lingnau, A., Pham, T. V., Hoffmann, S., Kubbutat, M. H., Jiménez, C. R., *J. Proteome Res.* 2010, *9*, 1913–1922.

[37] Tu, L. C., Yan, X., Hood, L., Lin, B., *Mol. Cell Proteomics* 2007, *6*, 575–588.

[38] Savola, S., Klami, A., Myllykangas, S., Manara, C., Scotlandi, K., Picci, P., Knuutila, S., Vakkila, J., *ISRN Oncol.* 2011, *2011*, 168712.

[39] Jafari, M., Primo, V., Smejkal, G. B., Moskovets, E. V., Kuo, W. P., Ivanov, A. R., *Electrophoresis* 2012, *33*, 2516–2526.

[40] Dhar, S. K., Lynn, B. C., Daosukho, C., St Clair, D. K., *J. Biol. Chem.* 2004, *279*, 28209–28219.

[41] Korgaonkar, C., Hagen, J., Tompkins, V., Frazier, A. A., Allamargot, C., Quelle, F. W., Quelle, D. E., *Mol. Cell Biol.* 2005, *25*, 1258–1271.

[42] Coffill, C. R., Muller, P. A., Oh, H. K., Neo, S. P., Hogue, K. A., Cheok, C. F., Vousden, K. H., Lane, D. P., Blackstock, W. P., Gunaratne, J., *EMBO Rep.* 2012, *13*, 638–644.

Published OnlineFirst May 30, 2013; DOI: 10.1158/0008-5472.CAN-12-3814

Molecular and Cellular Pathobiology

Cancer Research

PML-RARα and Its Phosphorylation Regulate PML Oligomerization and HIPK2 Stability

Yutaka Shima, Yuki Honma, and Issay Kitabayashi

Abstract

The *PML* gene is frequently fused to the *retinoic acid receptor α* (*RARα*) gene in acute promyelocytic leukemia (APL), generating a characteristic *PML-RARα* oncogenic chimera. PML-RARα disrupts the discrete nuclear speckles termed nuclear bodies, which are formed in PML, suggesting that nuclear body disruption is involved in leukemogenesis. Nuclear body formation that relies upon PML oligomerization and its stabilization of the hypoxia-inducible protein kinase (HIPK)-2 is disrupted by expression of the PML-RARα chimera. Here, we report that disruption of nuclear bodies is also mediated by PML-RARα inhibition of PML oligomerization. PKA-mediated phosphorylation of PML-RARα blocked its ability to inhibit PML oligomerization and destabilize HIPK2. Our results establish that both PML oligomerization and HIPK2 stabilization at nuclear bodies are important for APL cell differentiation, offering insights into the basis for the most common prodifferentiation therapies of APL used clinically. *Cancer Res; 73(14); 4278–88. ©2013 AACR.*

Introduction

In human leukemia, specific chromosomal translocations result in the expression of fusion proteins promoting malignancy (1, 2). The *PML* gene is the target of the t(15;17) chromosome translocation that is observed in more than 90% of acute promyelocytic leukemia (APL) cases, in which fusion of the *PML* and retinoic acid receptor α (*RARα*) genes leads to the expression of the aberrant PML-RARα fusion protein (3–6). The PML protein normally forms discrete nuclear speckles in the nucleus called PML nuclear bodies; in these, PML recruits other proteins, including transcription factors such as p53 and acute myeloid leukemia 1 (7–9), transcription coactivators such as hypoxia-inducible protein kinase (HIPK)-2 and p300 (10, 11), SUMO (12), and DAXX (13, 14). Nuclear bodies have been implicated in the regulation of apoptosis, cellular senescence, and antiviral responses. It has been reported that PML stabilizes transcription coactivators, such as HIPK2 and p300, to assemble transcription factor/coactivator complexes within nuclear bodies (15). In contrast, nuclear bodies are disrupted in t(15;17) APL (12, 16–19); in the presence of the PML-RARα fusion protein, nuclear bodies appear as dispersed microspeckles in which HIPK2 is destabilized (15). All-*trans*-retinoic acid (ATRA) and As_2O_3, which are used clinically in APL, restore the normal appearance of nuclear bodies (12, 17, 19–21). In t (15;17) APL, it remains unclear that the disruption of nuclear bodies is related to leukemogenesis and that their restoration would lead to therapy. The molecular mechanism by which PML-RARα disrupts nuclear bodies has remained elusive, hampering progress in the understanding of leukemogenesis.

The present study reveals that PML-RARα blocks PML oligomerization and disrupts nuclear bodies, and that the effect is reversed upon cAMP/PKA-dependent phosphorylation of PML-RARα. In addition, pharmacologic activation of adenylyl cyclase by forskolin restores PML nuclear bodies and promotes ATRA-induced APL cell differentiation. Furthermore, nuclear body restoration induced HIPK2 stabilization. These results suggest that nuclear body formation is regulated by PML-RARα phosphorylation, and that the restoration of nuclear bodies is important for APL cell differentiation.

Materials and Methods

Cell culture, infection, and antibodies

293FT cells, which were purchased from Invitrogen, and U2OS cells were cultured in Dulbecco's Modified Eagle Medium (DMEM) supplemented with 10% fetal calf serum (FCS). Plat-E cells were obtained from Dr. T. Kitamura (University of Tokyo, Tokyo, Japan) and were cultured in DMEM supplemented with 10% FCS, 10 μg/mL blasticidin, and 1 μg/mL puromycin. NB4 cells and K562 cells were cultured in RPMI-1640 medium supplemented with 10% FCS. Anti-HIPK2 antibody was described previously (15). Other antibodies were purchased commercially: anti-HA (3F10, Roche and Y11, Santa Cruz), anti-FLAG (M2, Sigma), anti-Myc (9E10, Upstate), anti-tubulin (H235, Santa Cruz), anti-PML (16.1–104, Upstate; H238, Santa Cruz; 001, MBL), anti-SUMO (Zymed), anti-DAXX (Exbio), and anti-RARα (C20, Santa Cruz).

Authors' Affiliation: Division of Hematological Malignancy, National Cancer Center Research Institute, Chuo-ku, Tokyo, Japan

Note: Supplementary data for this article are available at Cancer Research Online (http://cancerres.aacrjournals.org/).

Corresponding Author: Issay Kitabayashi, Division of Hematological Malignancy, National Cancer Center Research Institute, 5-1-1 Tsukiji, Chuo-ku, Tokyo 104-0045, Japan. Phone: 81-3-3547-5274; Fax: 81-3-3542-0688; E-mail: ikitabay@ncc.go.jp

doi: 10.1158/0008-5472.CAN-12-3814

Published OnlineFirst May 30, 2013; DOI: 10.1158/0008-5472.CAN-12-3814

Plasmids

The PML, PML-RARα, and HIPK2 expression vectors were generated as described previously (15). PML and PML-RARα deletion mutants were generated by PCR using pLNCX-HA-PML IV or pLNCX-HA-PML-RARα as the template.

Immunoprecipitation and Western blotting

293FT cells were transfected with the desired vectors and lysed as described previously (15). Cell lysates and immunoprecipitates were fractionated on SDS-polyacrylamide gels and transferred onto nitrocellulose membranes (Amersham). The membranes were incubated with primary antibodies and horseradish peroxidase-conjugated secondary antibodies. The immune complexes were visualized by the enhanced chemiluminescence (ECL) or ECL-Plus technique (Amersham), and the images were analyzed by ImageGauge (FUJIFILM).

Immunofluorescence

U2OS cells were cultured in 4-well chamber slides and transfected as described previously (15). The cells were exposed to 50 μmol/L forskolin for 18 hours. After forskolin exposure, the cells were fixed and incubated with antibodies as described previously. PML-RARα–expressing mouse c-kit$^+$ cells were exposed to 50 μmol/L forskolin for 24 hours. NB4 cells were exposed to 50 μmol/L forskolin or 1 μmol/L ATRA for 24 or 72 hours. The cells were analyzed by the same techniques as U2OS cells. Images were captured on an Olympus microscope and analyzed by deconvolution.

Serial replating assay

pMSCV, pMSCV-HA-PML-RARα, pMSCV-HA-PML-RARα ΔE, pMSCV-HA-PML-RARα S704A, pMSCV-HA-PML-RARα S704D, and pMSCV-HA-HIPK2 were transfected into Plat-E cells using GeneJuice (Novagen), and supernatants containing retrovirus were collected 48 hours after transfection. C-kit$^+$ cells were selected from the femurs of C57BL/6 mice using CD117-specific MicroBeads (Miltenyi Biotech), transduced with retroviruses using RetroNectin (Takara), and plated in methylcellulose medium (M3434, StemCell Technologies). The cells were cultured and replated every 4 to 6 days in methylcellulose medium under G418 selection. The cells from the first round (empty vector and PML-RARα ΔE) or the third round (PML-RARα point mutants) of colonies were harvested and analyzed by using immunofluorescence as described above. With respect to HIPK2 stabilization, c-kit$^+$ cells were infected with retroviruses containing HA-HIPK2. The next day, the cells were infected with retroviruses containing wild-type or mutants of HA-PML-RARα. The cells were cultured in methylcellulose medium under G418 and puromycin selection. The cells of the third-round colonies were harvested and subjected to Western blot analysis.

RT-PCR

Reverse transcriptase PCR was conducted as described previously (15). HIPK2 mRNA expression was analyzed using the following primers: forward (5′-CCCCTCAAATACATTCGCCC-3′) and reverse (5′-TGGTGTCTTCAGTCTCCACAAAGG-3′). The glyceraldehyde-3-phosphate dehydrogenase primer set was described previously (15).

Flow cytometric analysis

Before incubation with anti-Mac1-FITC (M1/70, eBioscience), NB4 cells were preincubated with immunoglobulin G from rat serum (Sigma) to prevent nonspecific binding of the antibody. The stained cells were analyzed by JSAN (Bay Bioscience), and the results were analyzed using FLOWJO software.

Results

PML oligomerization is required for nuclear body formation

The coiled-coil domain of PML mediates homo-oligomerization and hetero-oligomerization (18, 22–24). We have previously shown that PML IV interacts with 2 transcription factors important for granulocytic differentiation, PU.1 and CAAT/enhancer-binding protein (C/EBPε; refs. 25, 26). Therefore, we used PML IV and a PML mutant lacking the coiled-coil domain (PML IV ΔCC; Fig. 1A). As expected, PML IV ΔCC could not form homo-oligomers (Supplementary Fig. S1A). Immunofluorescence was conducted to assess the localization of the PML IV ΔCC mutant. As shown previously (21, 27), wild-type PML IV localized to the nucleus and formed nuclear bodies of normal appearance; however, the PML IV ΔCC mutant was expressed uniformly throughout the nucleus and did not form nuclear bodies (Supplementary Fig. S1B). These results suggest that PML oligomerization is associated with nuclear body formation. HIPK2 is stabilized by PML in nuclear bodies and destabilized by PML-RARα (15). To test whether the PML mutant destabilized HIPK2, FLAG-tagged HIPK2 was cotransfected with HA-tagged PML IV or PML IV ΔCC. Results showed that PML IV stabilized HIPK2, which is consistent with previous observations (15); however, PML IV ΔCC destabilized HIPK2 (Fig. 1B). The destabilization was rescued by a proteasome inhibitor, MG132 (Fig. 1B). These results suggest that PML oligomerization is required for PML-mediated HIPK2 stabilization.

PML-RARα disrupts nuclear bodies; however, the molecular mechanism underlying this effect remains unclear. The defect in nuclear body formation by the oligomerization-deficient PML IV ΔCC mutant led to the hypothesis that PML-RARα may prevent PML oligomerization. To test this hypothesis, the effect of PML-RARα on nuclear body disruption was evaluated by immunofluorescence. Wild-type PML and PML-RARα are expressed in APL cells. The localization of PML is diffused in cells expressing PML-RARα (18). We transfected U2OS cells with expression vectors encoding FLAG-tagged PML IV and hemagglutinin (HA)-tagged PML IV or HA-tagged PML-RARα. PML nuclear bodies were detected using anti-FLAG antibody. As shown in Supplementary Fig. S2B, PML IV formed large, discrete, and distinct nuclear foci in the absence of PML-RARα (top) but small and disperse foci in the presence of PML-RARα (bottom). The oligomerization capacity of PML was subsequently assessed in the presence and absence of PML-RARα. As shown in Supplementary Fig. S2C, PML-RARα inhibited PML–PML interaction, suggesting

Published OnlineFirst May 30, 2013; DOI: 10.1158/0008-5472.CAN-12-3814

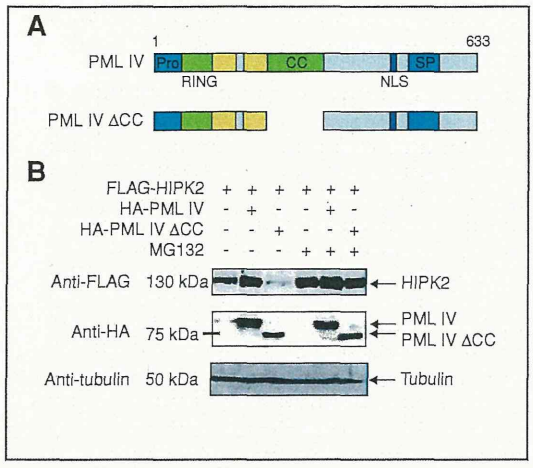

Figure 1. The coiled-coil domain of PML is required for HIPK2 stabilization. A, diagram of the PML deletion mutant. The proline-rich region (Pro), the ring-finger domain (RING), the coiled-coil domain (CC), the nuclear-import signal (NLS), and the serine-proline–rich region (SP) are indicated. B, PML IV ΔCC destabilizes HIPK2. 293FT cells were transfected with pLNCX-FLAG-HIPK2 and empty vector, pLPCX-HA-PML IV, or pLPCX-HA-ΔCC. The cells were treated with or without 10 μmol/L MG132 for 16 hours. The expression of HIPK2 (top), PML IV, or PML IV ΔCC (middle) and tubulin (bottom) was detected by immunoblotting using anti-FLAG, anti-HA and anti-tubulin antibodies, respectively.

that PML-RARα disrupts PML nuclear bodies by inhibiting PML oligomerization. The N-terminal or the coiled-coil domain of PML-RARα has been reported to be important for nuclear body disruption (28). PML 1–394, which is the PML moiety of PML-RARα and lacks the PML C-terminal, did not disrupt PML nuclear bodies (Supplementary Fig. S2D), suggesting that the RARα moiety of the fusion protein is also important for nuclear body disruption.

The ligand-binding domain of the RARα moiety of PML-RARα is essential for nuclear body disruption

Because the RARα moiety of PML-RARα is important for the disruption of PML nuclear bodies, PML-RARα deletion mutants were generated (Fig. 2A) to identify the region of RARα required for the effect. HA-tagged deletion mutants were cotransfected with FLAG-tagged PML IV. Immunofluorescence analysis indicated that PML-RARα 1–748 led to dispersed microspeckles, as did wild-type PML-RARα, but that deletion mutants lacking the ligand-binding domain, such as PML-RARα 1–567, 1–492, and 1–420, did not (Fig. 2B). These results suggest that the ligand-binding domain of RARα plays an important role in PML-RARα–mediated nuclear body disruption. The ΔE PML-RARα mutant, which lacks the ligand-binding domain (Fig. 2A), failed to disrupt nuclear bodies (Fig. 2B). The ΔC PML-RARα mutant, which lacks the DNA-binding domain, disrupted nuclear bodies (Fig. 2B). All of the PML-RARα deletion mutants were expressed at similar levels (Fig. 2C). We also tested the effect of the wild-type PML-RARα and the ΔE PML-RARα mutant on endogenous nuclear body formation in normal myeloid stem/progenitor cells. As the cells transduced with PML-RARα ΔE were not immortalized (Fig. 2D), we assayed for PML localization using the cells of first-round colonies with an anti-PML antibody specific for mouse Pml. Nuclear bodies were not disrupted in PML-RARα ΔE–infected cells (Fig. 2E). The localization of ΔE was different from that of wild-type PML-RARα. The ligand-binding domain of PML-RARα might be important for its dispersion. These results suggest that the ligand-binding domain of PML-RARα is indeed important for nuclear body disruption.

The effect of these PML-RARα mutations on HIPK2 stability was assessed. As shown in Fig. 2F, wild-type PML-RARα and PML-RARα 1–748, which disrupted nuclear bodies, destabilized HIPK2, whereas the other PML-RARα mutants, which did not disrupt nuclear bodies, did not destabilize HIPK2. To assess the effect of the same PML-RARα mutations on PML oligomerization, 293FT cells were cotransfected with Myc-tagged and FLAG-tagged PML IV together with HA-tagged PML-RARα mutants. As shown in Fig. 2G, immunoprecipitation and Western blotting indicated that wild-type PML-RARα and 1–748 inhibited the interaction between Myc-tagged and FLAG-tagged PML, whereas the other PML-RARα mutants did not. These results support the essential role of the ligand-binding domain of PML-RARα in the disruption of PML nuclear bodies.

The PKA phosphorylation site of PML-RARα is required for nuclear body disruption

Experiments were carried out to identify the sites responsible for PML nuclear body inhibition within the ligand-binding domain. As shown in Supplementary Fig. S3A, HA-tagged PML-RARα 1–708 or 1–661 was cotransfected with FLAG-tagged PML IV. PML-RARα 1–708 led to the formation of microspeckle PML nuclear bodies, whereas PML-RARα 1–661 did not (Supplementary Fig. S3B). These results indicate that the PML-RARα region spanning amino acids 662 to 708 is required for PML nuclear body inhibition. RARα and PML-RARα are phosphorylated by PKA (29, 30). Because serine 704, the PKA-dependent phosphorylation site of PML-RARα, is located within the region required for nuclear body disruption (Fig. 3A), mutants were generated in which serine 704 was substituted by alanine and aspartate to simulate dephosphorylated and phosphorylated serine, respectively. The effect of these mutants on PML nuclear body formation was assessed by the transfection of U2OS cells. Representative immunofluorescence data are shown in Fig. 3B (left), and the expression levels of PML and PML-RARα are shown in Fig. 3C. Quantification was done by counting the number of cells that formed large, discrete, and distinct PML nuclear foci in all transfected cells (Fig. 3D). Interestingly, wild-type PML-RARα and the alanine mutant (S704A) disrupted nuclear bodies, as shown by the presence of microspeckles, whereas the aspartate mutant (S704D) did not. Both mutants interacted with PML IV as strongly as did wild-type PML-RARα and the ΔE mutant (Supplementary Fig. S4), suggesting that the inability to disrupt nuclear bodies is not due to any deficiency in binding to PML. Forskolin was then used to activate adenylyl cyclase to

Published OnlineFirst May 30, 2013; DOI: 10.1158/0008-5472.CAN-12-3814

determine whether cAMP/PKA might restore nuclear bodies by phosphorylating the serine residue of PML-RARα. In the presence of forskolin, wild-type PML-RARα did not affect nuclear bodies (Fig. 3B and D); however, the S704A mutant, which lacks the serine residue phosphorylated by PKA, inhibited PML nuclear body formation even in the presence of forskolin.

We also tested the effect of wild-type and mutant PML-RARα in normal myeloid stem/progenitor cells. C-kit$^+$ mouse myeloid stem/progenitor cells were infected with a retrovirus encoding HA-tagged PML-RARα, HA-tagged S704A, or HA-tagged S704D and cultured in methylcellulose medium. The location of Pml in the immortalized cells was assessed using an anti-PML antibody specific for mouse Pml. Representative immunofluorescence data are shown in Fig. 4A, and quantification is shown in Fig. 4B. Nuclear body formation was maintained in S704D-expressing cells but was largely disrupted in wild-type PML-RARα- and S704A-expressing cells. The cells transduced with S704D were immortalized as well as those transduced with PML-RARα and S704A (Fig. 4C). Wild-type PML-RARα, S704A, and S704D were expressed at similar levels in the immortalized cells (Fig. 4D). Forskolin restored PML nuclear bodies in the wild-type PML-RARα–expressing cells but could hardly restore nuclear bodies in the S704A-expressing cells (Fig. 4E). These results suggest that the ability of PML-RARα to disrupt nuclear bodies is inhibited by cAMP/PKA-mediated phosphorylation of PML-RARα at serine 704.

Disruption of PML nuclear bodies by PML-RARα is strongly correlated with the destabilization of HIPK2 and the inhibition of PML oligomerization by PML-RARα

As shown in Fig. 1B and Supplementary Fig. S1B, PML IV ΔCC did not form nuclear bodies and destabilized HIPK2. Similarly, the PML-RARα deletion mutants that inhibited PML nuclear body formation also destabilized HIPK2 (Fig. 2F). These results suggest a correlation between nuclear body formation and HIPK2 stability. Therefore, the PML-RARα point mutants described above were assessed for their effect on HIPK2 stability. As shown in Fig. 5A, the level of HIPK2 decreased when HIPK2 was cotransfected with wild-type PML-RARα or S704A but not when HIPK2 was cotransfected with S704D. The effect of the point mutants on HIPK2 stability was also assessed in a stable system as shown in Fig. 4. Endogenous mouse HIPK2 could not be detected (data not shown). The expression of HA-tagged human HIPK2, introduced in mouse c-kit$^+$ cells, was detected only in S704D-expressing cells (Fig. 5B) of the third-round colonies. However, HIPK2 mRNA levels in cells expressing wild-type PML-RARα, S704A, or S704D were not appreciably different (Supplementary Fig. S5). These data support the hypothesis that HIPK2 destabilization is associated with PML nuclear body disruption. The point mutants were then assessed for their effect on PML oligomerization. S704A inhibited PML homo-oligomerization, as did wild-type PML-RARα, whereas S704D did not (Fig. 5C), implying that the protection of PML oligomerization from PML-RARα promotes PML nuclear body formation.

PKA-dependent phosphorylation of PML-RARα restores nuclear bodies and promotes ATRA-induced APL cell differentiation

As shown in Figs. 3–5, PKA-dependent phosphorylation of PML-RARα may be the switch that restores nuclear bodies. Cyclic AMP (cAMP) alone has no effect on nuclear body restoration, but cAMP and ATRA cooperatively restore nuclear bodies in NB4-R1 cells, which are ATRA-maturation–resistant cell lines (31). These data suggest that the cAMP/PKA pathway plays an important role in nuclear body formation. To determine whether the cAMP/PKA pathway actually regulates nuclear body formation in APL cells, APL-derived NB4 cells, which express endogenous PML-RARα, were exposed to forskolin alone. Nuclear bodies were detected using an anti-PML antibody; nuclear bodies were disrupted in NB4 cells, and became clear in the presence of forskolin (Supplementary Fig. S6A). Forskolin did not induce NB4 cell differentiation (Supplementary Fig. S6A). To characterize the forskolin-induced clear particles, the localization of SUMO and DAXX, which are recruited to nuclear bodies, was assessed using anti-SUMO and anti-DAXX antibodies. In the absence of forskolin or ATRA, the colocalization of SUMO and PML, or DAXX and PML, was very limited (Supplementary Fig. S6B). In contrast, ATRA restored nuclear bodies and recruited SUMO and DAXX to nuclear bodies. Forskolin changed the appearance of PML nuclear bodies from microspeckles to clear particles. In the clear particles, PML colocalized with SUMO and DAXX (Supplementary Fig. S6B). Thus, forskolin alone, like ATRA, restored nuclear bodies. ATRA induced PML-RARα degradation, whereas forskolin did not (Supplementary Fig. S6C). These data might reflect the smaller size of nuclear bodies in the presence of forskolin compared with that of ATRA. These data also suggest that PML-RARα phosphorylated by cAMP/PKA inhibits nuclear body disruption.

Because forskolin restored nuclear bodies in NB4 cells, the stability of endogenous HIPK2 was assessed in NB4 cells exposed to forskolin. As shown in Fig. 6A, forskolin increased HIPK2 protein levels but not HIPK2 mRNA levels. In contrast, forskolin did not increase HIPK2 protein levels in the non-APL K562 cells (Fig. 6B). HIPK2 protein levels increased in NB4 cells exposed to ATRA for 24 hours (Fig. 6C). Time-course analysis indicated that the increase in HIPK2 expression was correlated with nuclear body restoration (Fig. 6C and D). These results suggest that HIPK2 is stabilized in nuclear bodies restored upon cAMP/PKA-mediated phosphorylation of PML-RARα.

Finally, NB4 cells were exposed to forskolin or/and ATRA to determine whether nuclear body restoration may promote NB4 cell differentiation. As shown previously, forskolin was not sufficient to induce NB4 cell differentiation (Fig. 6E and F); however, forskolin enhanced ATRA-induced differentiation (Fig. 6E and F). The combination of ATRA and forskolin resulted in the differentiation of NB4 cells into segmented granulocytes (Fig. 6F) and increased the expression of the differentiation marker Mac-1 (Fig. 6G) more efficiently than either drug alone. Other studies have also shown the efficacy of cAMP against APL (32–35). These results and reports suggest that cAMP/PKA promotes ATRA-induced APL cell differentiation by restoring nuclear bodies.